Prediction of the continuous probability of sand screen-out based on a deep learning workflow

Lei Hou [a, *], Yiyan Cheng [b], Derek Elsworth [c], Honglei Liu [d], Jianhua Ren [b]

[a] School of Engineering, The University of Warwick, Coventry CV4 7AL, UK

[b] Research Institute of Exploration & Development, East China Company of SINOPEC, Nanjing 210011, China

[c] Energy and Mineral Engineering, EMS Energy Institute and G3 Center, Pennsylvania State University, University Park, 16802, USA

[d] SINOPEC Research Institute of Petroleum Engineering, Beijing 100101, China

Abstract

Sand screen-out is one of the most serious and frequent challenges that threaten the efficiency and safety of hydraulic fracturing. Current low prices of oil/gas drive operators to control costs by using lower viscosity and lesser volumes of fluid for proppant injection - thus reducing the sand-carrying capacity in the treatment and increasing the risk of screen-out. Current analyses predict screen-out as isolated incidents based on the interpretation of pressure or proppant accumulation. We propose a method for continuous evaluation and prediction of screen-out by combining data-driven methods with field measurements recovered during shale gas fracturing. The screen-out probability is updated, redefined and used to label the original data. Three determining elements of screen-out are proposed, based on which four indicators are generated for training a deep learning model (GRU – Gated Recurrent Units, tuned by the Grid search and Walk-forward validation). Training field records following screen-out are manually trimmed to force the machine learning algorithm to focus on the pre-screen-out data, which then improves the prediction of the continuous probability of screen-out. The Pearson coefficients are analyzed in the STATA software to remove obfuscating parameters from the model inputs. The extracted indicators are optimized, *via* a forward selection strategy, by their contributions to the prediction according to the confusion matrix and root mean squared error (RMSE). By optimizing the inputs, the probability of screen-out is accurately predicted in the testing cases, as well as the precursory predictors, recovered from the probability evolution prior to screen-out. The effect of pump rate on screen-out probability is analyzed, defining a U-shaped correlation and suggesting a safest-fracturing pump rate (SFPR) under both low- and high-stress conditions. The probability of screen-out and the SFPR, together, allow continuous monitoring in real-time during fracturing operations and the provision of appropriate screen-out mitigation strategies.

Keywords: hydraulic fracturing; screen-out; deep learning; continuous probability; pump rate

* Corresponding author.
E-mail address: lei.hou@warwick.ac.uk (L. Hou).

1 Introduction

Sand screen-out occurs where the proppant in the fracturing fluid creates a bridge across the evolving fluid-driven fracture, constricts the flow area (eg. the perforation hole, fractures, etc.) and results in a rapid rise in injection pressure during hydraulic fracturing (Sun et al. 2020; Economides and Nolte 1989). Screen-out is considered to be one of the most serious problems that threaten the safety of equipment and individuals during fracturing, reduce the stimulated production and result in cost overruns due to the time and material consumption related to wellbore clean-up operations and equipment maintenance (Cleary et al. 1993; E.V. Dontsov and Peirce 2014).

Previous research on the fracturing of conventional reservoirs suggests that the near-wellbore tortuosity of fractures may play an important role in causing screen-out, in addition to fluid leak-off, proppant beach-formation and other factors, according to experiments and field measurements (Barree and Conway 2001; Aud et al. 1994; Daneshy 2007). Based on these mechanisms, screen-out may be potentially predicted by interpreting time histories of fracturing pressure based on log-log plots (Nolte and Smith 1981), calculating the configuration of the proppant distribution in fractures (Cai et al. 2017), diagnosing the connection between wellbore and formation through the perforations based on acoustic measurements (Merry and Dalamarinis 2020), or inspecting the variation with time of the treatment pressures (Massaras and Massaras 2012), among other indicators. Data-driven approaches have also been introduced for prediction by integrating the inverse slope method with deep learning algorithms (CNN-LSTM) (Sun et al. 2020), predicting the fracturing pressure using the locally-weighted linear regression and CNN-RNN (J. Hu et al. 2020; Ben et al. 2020), and learning pre-screen-out patterns in the simulated pressure signals (Yu, Trainor-Guitton, and Miskimins 2020).

For unconventional reservoirs, the screen-out mechanism may be more complex, due to larger volumes of injection, higher pumping rates, elevated injection pressures and multi-staged operations in the horizontal wellbore (Weng et al. 2011; Li et al. 2015). The resulting complex fracture networks, compared with the single high-conductivity bi-wing fracture typical in conventional vertical wells, are required to maximize the stimulated reservoir volume (Warpinski et al. 2009; Qi et al. 2012). The pressure fluctuations are also more severe than in conventional reservoirs. Rapid rises and drops in

pressure are commonly observed in shale gas fracturing (Roussel, Manchanda, and Sharma 2012), making the previous recovery of diagnostics from the pressure curve more difficult to recover. Besides, most of the previous efforts provide the screen-out prediction as a discrete classification result (i.e. screen-out or non-screen-out). The sudden appearance doesn't reflect the inducements before the screen-out and also may reserve limited time for the operator to make judgments and adjustments.

We, therefore, focus on the continuous diagnosis of screen-out by field data processing, attempting to improve the fidelity of the early warning and define the form of signals that are precursory and robustly diagnostic of an impending incident. Since mild screen-out could be useful in increasing the net pressure in the driven fracture and thereby enhance the stimulated volume of the reservoir (Massaras and Massaras 2012; E. Dontsov and Peirce 2015), the definition of screen-out is first constrained into the most critical level where fracturing operations are suspended in the open well by the release of pressure and cleaning of the wellbore is mandated. The determining-element mechanisms of screen-out are proposed and used to redefine and label the screen-out probability, which considers a greater number and broader variety of influence factors compared with previous efforts that have mainly relied on pressure interpretation or proppant accumulation (Massaras and Massaras 2012; Cai et al. 2017). The pump rate, one of the determining elements, is fitted for the safest value where the probability of screen-out approaches the minimum. STATA software is used for the optimization of the model inputs with a deep learning workflow trained then tested against rigorously selected field examples with known outcomes. The resulting continuous screen-out probability monitoring and the safest fracturing pump rate may then be used to improve early warning of screen-out and allow mitigation in real-time to promote safe and efficient fracturing operations.

2 Methodology

New hypotheses of screen-out are proposed to redefine the screen-out probability and extract indicators for the screen-out predicting. In this work, the definition of screen-out is constrained to the most serious condition where open-well flushing is necessary – since this is the basis on which our

field cases are collected. STATA software and a GRU model are applied to these datasets for parameter analyses and predictions of screen-out probability.

2.1 Hypotheses of screen-out

(i) Determining elements hypothesis: Three determining elements of screen-out for shale gas fracturing are proposed – namely, pump rate, fracture volume/capacity and proppant accumulation (Novotny 1977; Patankar et al. 2002; Dahi-Taleghani and Olson 2011; Aud et al. 1994). The mechanism of screen-out is presumed to result from parameter mismatch among the determining elements. New indicators are generated based on the element hypothesis to aid machine interpretation of the raw data. Screen-out probability is redefined by fixing two of the elements.

(ii) Linear-correlation hypothesis: For shale gas fracturing, the pump rate for proppant injection is near-constant. We assume that the probability of screen-out has a linear relationship with the injected volume of proppant under constant pump rate and fixed fracture capacity. Then, the screen-out probability is defined as the ratio of injected proppant volume to the maximum capacity (total cumulative volume of injected proppant before the restricted screen-out), which is then used to label the original data. According to this hypothesis, the ideal screen-out probability curve (probability-*vs*-fracturing time) is a smooth and continuous increasing line. However, the fracture is considered to continue propagating during the fracturing operation, which results in a continuous increase in fracture volume with time (Manchanda et al. 2020; Dahi-Taleghani and Olson 2011). Therefore, the actual probability may fluctuate regularly around the ideal curve, but with relatively small departures, due to this continuing fracture propagation.

2.2 Data preparation

2.2.1 Data collection

The field data are collected based on the restricted definition of screen-out (the fracturing operation is suspended to release pressure and clean the wellbore). 25 stages of fracturing data are collected from shale gas wells in the Sichuan basin, China, including ~120,000 groups of field measurements. The parameters in each group consist of both the geological features (well depth, vertical depth, minimum horizontal stress) and treatment/fracturing records (pump rate, fluid and proppant type, wellhead pressure, proppant concentration, shut-in pressure and stage length). The

original fluid and proppant types are non-numeric parameters and are replaced by the fluid viscosity and proppant diameter, as representative parameters of performance, respectively.

The data are split into the training (21 stages) and testing datasets (4 stages) for model training and prediction, as shown in Table 1. The testing stages are rigorously selected by well locations. The geological and in-situ stress conditions vary as the increasing well distance, which may increase the difficulty of model prediction, thus providing a more reliable evaluation of the model performance and application range. One of them is from the same well (Well A) that is also used for model training. The other three stages come from new wells different from the training wells, one of which is from a neighbouring well (Well B), and the other two from remote wells (Wells C and D are more than 200 km distant from all other wells). All wells, noted in Table 2, are drilled within the same formation.

Table 1 Division of training and testing datasets

	Training sets / stage	Testing sets / stage	Notes
Training wells	21	/	/
Well A	/	1	From one of the training wells
Well B	/	1	From a neighbouring well next to training wells
Well C	/	1	From a well in a different location of the basin
Well D	/	1	

2.2.2 Data labelling, trimming and extracting

Screen-out probability is calculated and used to label the original field measurements according to our most severe definition. We truncate the field record following screen-out to direct the machine to the experience pre-screen-out. Although the training results may be influenced by the missing data, it boosts the interpretation of the pre-screen-out data, then benefits the continuous monitoring for the generation of screen-out. It may also prevent the model from cheating by recognizing the overpressure or pump-off for screen-out, which bypasses the deeper interpretation of data. Similar data processing is also reported by previous research (Yu, Trainor-Guitton, and Miskimins 2020).

Four new indicators of screen-out are proposed based on the element hypothesis to assist the model prediction – the downhole pressure after hole perforation (*DPP*), the ratio of the accumulated

volume of injected proppant to that of injected fluid (V_s/V_f), the wellhead pressure change in a unit volume of injected fluid ($\Delta P/\Delta V_f$) and the ratio of minimum-horizontal stress to shut-in wellhead pressure (σ_{min}/P_s). The *DPP*, calculated from the wellhead pressure, may reflect the pressure variation induced by fracture propagation and new fracture generation (E.V. Dontsov and Peirce 2014; Willingham, Tan, and Norman 1993). Details of pressure conversion can be found in Appendix A. The V_s/V_f ratio represents proppant accumulation in fractures. The $\Delta P/\Delta V_f$ ratio is similar to the pressure slope returned under a constant pump rate (Massaras and Massaras 2012). The σ_{min}/P_s ratio reflects the change in in-situ stress due to the material injection (Hayashi and Haimson 1991).

2.3 Data processing tools

The parameter analyses are carried out in STATA 17.0 to assist the selection of model inputs. The data training and testing are performed using a GRU model built in the Spyder environment. The GRU algorithm, designed for extracting information from time sequences (Cho et al. 2014), has performed well in various petroleum engineering applications (Wang et al. 2019; Sun et al. 2020). According to previous experience (Fan et al. 2021; Sagheer and Kotb 2019), a three-layer (including the output layer) GRU is established with the activation function 'ReLu' operating in each layer (Gal and Ghahramani 2015). The regularization is performed to avoid overfitting by setting a dropout rate (of 0.2) behind the first and hidden layers. The 'Adam' is selected as the optimizer to compile the model, where a callback function is applied to return and automatically update the learning rate (Kingma and Ba 2014; Zeiler 2012). Other hyperparameters, including the number of neural units (30), epochs (30) and batch size (100) are optimized by the Grid search and Walk-forward validation (Bergstra and Bengio 2012; M.Y. Hu et al. 1999; Stein 2002). Details of model tuning can be found in Appendix B.

The workflow of data processing is graphically illustrated in Fig. 1. The original field measurements and extracted indicators are analyzed by the Pearson correlation coefficients in STATA. The GRU model is initially trained using the selected original parameters, and the results are used as a reference. The indicators are appended to the inputs successively for optimization based on the forward selection strategy. The model performance is promoted by indicator optimization and is verified by the testing cases. The deep learning workflow proposed in this study has high feasibility

for different application scenarios if provided with the corresponding datasets for the model training. It is also possible to promote the performance of the workflow by feeding into new data.

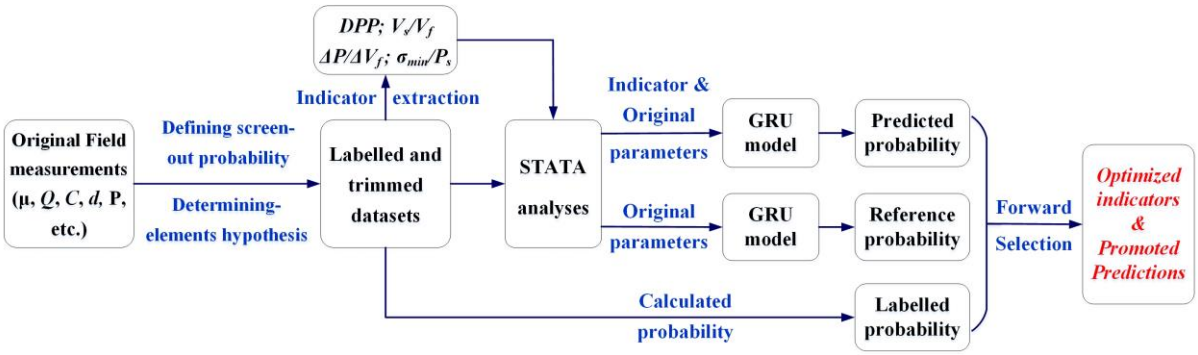

Fig. 1 The workflow of data processing, consisting of data collection, pre-processing and model training.

3 Results

Interfering parameters are removed from the model inputs according to the Pearson coefficient analyses. The confusion matrix and the root mean squared error (RMSE) are used as criteria for the model evaluation, in which the RMSE has the same unit as the prediction (Chai and Draxler 2014). The optimized indicators improve the prediction by halving the reference RMSE and eliminating the false-negative errors. Successful reports of screen-out and accurate predictions of its probability are achieved – and may be used in continuous monitoring of fracturing operations.

3.1 Pearson correlation coefficient analyses

The Pearson correlation coefficient is the covariance of the two variables divided by the product of their standard deviations and is used to quantify the potential interference between variables (Benesty et al. 2009). The inputs of the deep learning model are analyzed in STATA, and the results are summarized in Table 2. The higher the coefficient is, the stronger the interference that may exist between the two variables. Using the coefficient as a reference, we remove the variable that may significantly interfere with other multiple variables. The Well depth shows high coefficients with the Vertical depth and Stage length, as well as the Vertical depth with Minimum-horizontal-stress, Wellhead pressure and DPP. Therefore, the Well depth and Vertical depth are removed from the inputs of the model training.

The optimization of model inputs is performed with care and with appropriate reference to engineering experience and preserving as much parameter/information as possible for the GRU

neuronal units. For instance, the large coefficient linking proppant diameter and proppant concentration may be due to the characteristics of the data (they are always present in pairs). These variables are reserved because the diameter and concentration of proppant may each contribute to screen-out but by different mechanisms (sealing the hydraulic fracture alternately by bridging or filling, respectively.). There is also a concern that removing the proppant-related features may mislead future works when collecting the original data.

Table 2 The Pearson correlation coefficients between training variables

	(1)	(2)	(3)	(4)	(5)	(6)	(7)	(8)	(9)	(10)	(11)	(12)	(13)	(14)
(1)	1													
(2)	**0.64**	1												
(3)	0.10	0.44	1											
(4)	**-0.77**	-0.43	0.30	1										
(5)	0.13	-0.04	-0.15	-0.20	1									
(6)	-0.08	-0.15	-0.14	0.04	-0.21	1								
(7)	-0.11	-0.06	0.02	0.14	-0.24	0.51	1							
(8)	-0.09	-0.06	0.02	0.11	-0.25	0.50	0.80	1						
(9)	0.47	**0.70**	0.47	-0.18	-0.06	0.25	0.12	0.16	1					
(10)	0.30	**0.74**	0.58	0.00	-0.02	-0.43	-0.19	-0.15	0.71	1				
(11)	-0.17	0.03	0.12	0.23	-0.37	0.67	0.54	0.57	0.35	-0.04	1			
(12)	0.02	0.02	-0.01	-0.01	-0.01	-0.04	-0.02	-0.02	-0.02	0.01	-0.02	1		
(13)	0.43	**0.83**	0.47	-0.10	-0.07	-0.16	-0.04	-0.05	0.71	0.80	0.05	0.02	1	
(14)	-0.03	0.07	0.02	0.01	-0.31	0.55	0.41	0.49	0.41	0.02	0.86	-0.02	0.04	1

Notes: The original measurements: (1) Well depth; (2) Vertical depth; (3) Min-horizontal stress; (4) Stage length; (5) Fluid viscosity; (6) Pump rate; (7) Proppant concentration; (8) Proppant diameter; (9) Wellhead pressure. The extracted indicators: (10) DPP; (11) V_s/V_f; (12) $\Delta P/\Delta V_f$; (13) σ_{min}/P_s. The dependent variable: (14) Screen-out probability.

3.2 Screen-out prediction based on original measurements

The original field measurements, parameters (3) to (9) in Table 2, are used as inputs to the GRU model for screen-out probability prediction. The results are shown in Fig. 2, where the time histories of pump rate, proppant concentration and wellhead pressure are also presented. The confusion matrix and the RMSE are used as dual criteria for evaluating the predictions. We define that a predicted screen-out probability higher than 0.9 generates a report of screen-out. The workflow based on the original parameters fails to give the correct screen-out warning in three of four testing cases. Three false-negatives (FN error, in Wells A, C and D cases, as shown in Figs. 2 a, c and d), four false-positives (FP error, in Wells B and D cases, as shown in Figs. 2 b and d) and only one correct

prediction are reported, as shown in Table 3. There is essentially no pattern for the predicted curves that produce RMSEs of 0.230 (Well A), 0.236 (Well B), 0.150 (Well C) and 0.369 (Well D), respectively, compared with the labelled probability.

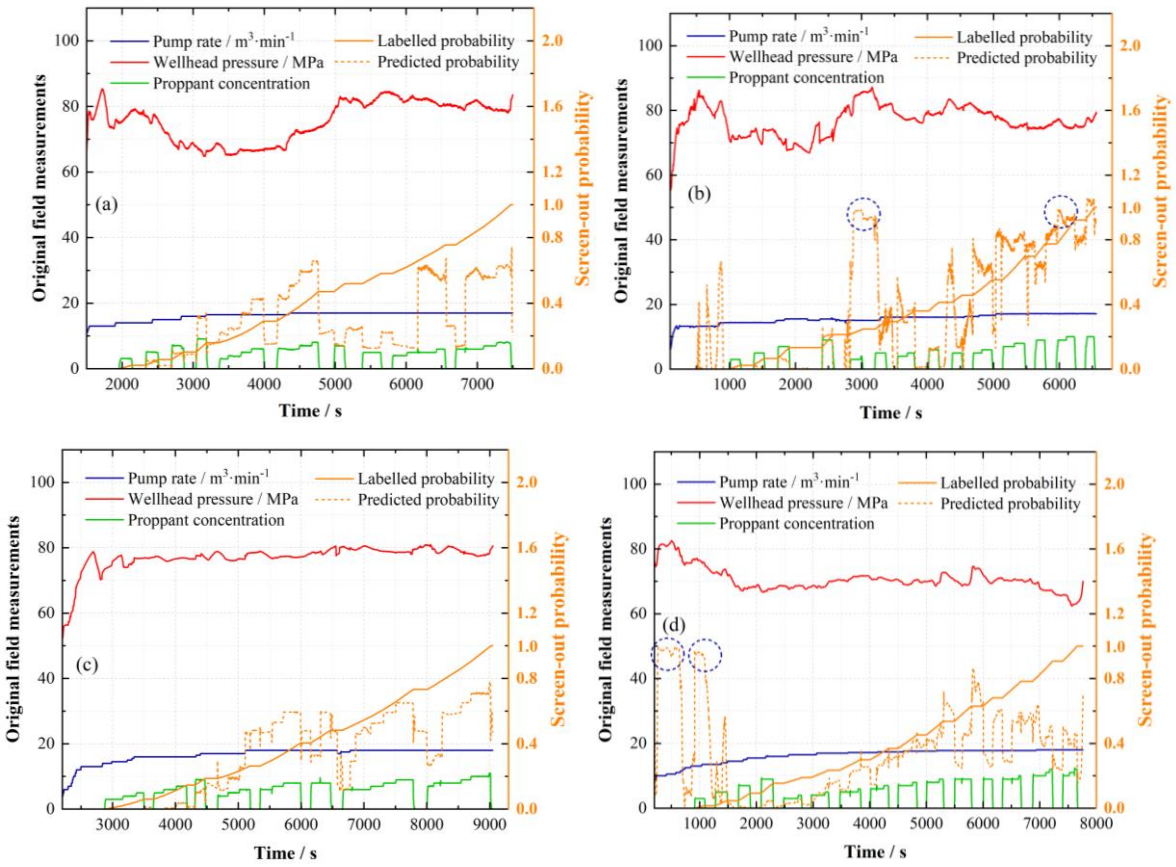

Fig. 2 Prediction of screen-out probability using the original measurements from (a) Well A, (b) Well B, (c) Well C and (d) Well D. The blue dashed circle marks the false alarm of screen-out in Wells B and D. The solid orange line is the labelled screen-out probability curve. The dashed line is the predicted probability curve. The wellhead pressure, pump rate, proppant concentration are presented to show the operation procedures.

Table 3 The confusion matrix of the predictions based on original parameters

		Predicted events	
		Screen-out	**Non-screen-out**
Actual events	**Screen-out**	1 (Correct)	3 (FN error)
	Non-screen-out	4 (FP error)	/

3.3 Prediction promotion by optimizing indicators

The predictions are improved by optimizing the extracted indicators compared with the results based on original measurements. The forward selection strategy is applied for the optimization, during which the indicator is appended sequentially to the model inputs. The primary indicator that promotes the prediction is selected, and the others decreasing model performance are abandoned.

The first testing indicator is decided by regression analyses using the OLS (ordinary least squares) method (executed in STATA) to produce the best prediction with the least indicators. The results are summarized in Table 4. The V_s/V_f ratio increases the R-squared value more than do the other indicators (from 0.483 to 0.799), indicating the most significant contribution of V_s/V_f to the screen-out probability prediction. Therefore, the V_s/V_f is chosen as the first testing parameter for the forward selection.

Table 4 Regression results between indicators and screen-out probability

Dependent variable	Screen-out probability						
Independent variables	*DPP*		-0.001				-0.005
	V_s/V_f			21.669			21.914
	$\Delta P/\Delta V_f$				0.000		0.000
	σ_{min}/P_s					-0.473	-0.257
Control variables	Min-horizontal stress	-0.013	-0.01	-0.012	-0.013	-0.013	-0.012
	Stage length	0.002	0.003	-0.005	0.002	0.003	-0.003
	Fluid viscosity	-0.005	-0.005	-0.001	-0.005	-0.005	-0.002
	Pump rate	0.016	0.013	-0.008	0.016	0.009	-0.024
	Proppant concentration	-0.005	-0.005	-0.012	-0.005	-0.002	-0.010
	Proppant diameter	0.709	0.707	0.283	0.709	0.641	0.233
	Wellhead pressure	0.008	0.010	0.003	0.008	0.013	0.012
Constant		0.328	0.328	0.328	0.328	0.328	0.328
R-squared		**0.483**	**0.483**	**0.799**	**0.483**	**0.513**	**0.821**

The results of the forward selection are presented in Table 5, using the confusion matrix and RMSE as the dual criteria. The introduction of V_s/V_f boosts the model performance by significantly reducing the RMSE and increasing the number of correct predictions by a single instance. The combination of V_s/V_f and *DPP* in the second round selection predicts the ultimate occurrence of screen-out events in three of four testing cases and halves the number of false-positives. By adding the $\Delta P/\Delta V_f$ ratio, the workflow successfully reports all of the screen-out events and produces the lowest RMSE in all testing rounds. Therefore, the indicators in the first three rounds are all selected. The

σ_{min}/P_s in the last round is abandoned due to the increasing RMSE and false-negative error, as shown in Table 5.

Table 5 Results of the indicator optimization by the forward selection

Forward selection	Indicators appended to model inputs	FP error	FN error	Correct report /Total event	Averaged RMSE	Decision
Reference	/	4	3	1/4	0.246	/
Round 1	V_s/V_f	4	2	2/4	0.176	Selected
Round 2	V_s/V_f + DPP	2	1	3/4	0.130	Selected
Round 3	V_s/V_f + DPP + $\Delta P/\Delta V_f$	3	0	4/4	0.089	Selected
Round 4	V_s/V_f + DPP + $\Delta P/\Delta V_f$ + σ_{min}/P_s	6	0	4/4	0.126	Abandoned

The predictions in the third-round test are shown in Fig. 3. Three false-positives are observed for Wells C and D that are located distant from the training cases (wells), as marked by dashed circles in Figs. 3 (c) and (d). The false-positive error (the false alarm) is considered less serious than the false-negative error (the missing alarm) (Pounds and Morris 2003). Besides, the false alarms are reported at the end of the fracturing operation, and about 15 minutes ahead of the actual screen-out, which may be acceptable. Therefore, the GRU-based workflow, trained by the original and extracted parameters, reports accurate screen-out warnings and exerts stable performance in rigorous applications. The continuous monitoring of screen-out probability allows the field operator to receive pre-warning and allow rapid response in near-real-time, which is more efficient and practical than the previous discrete predictions.

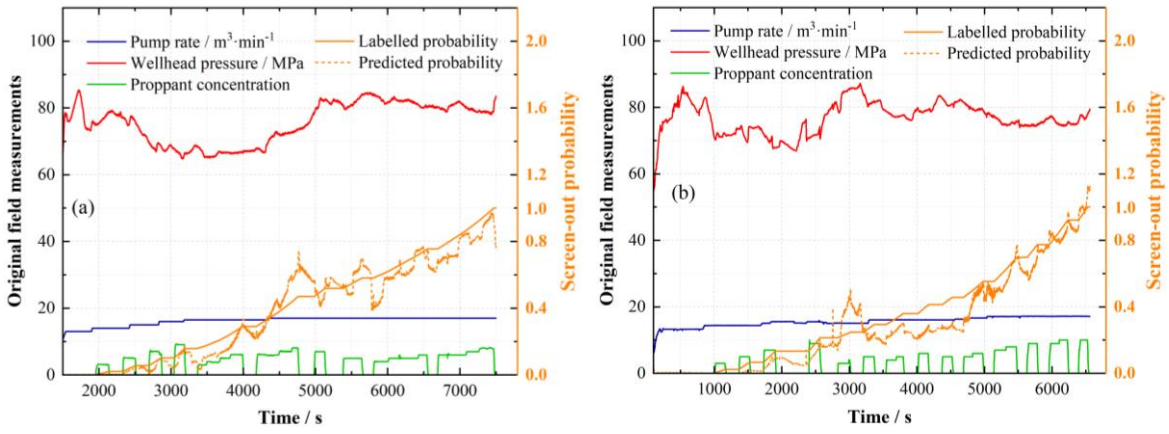

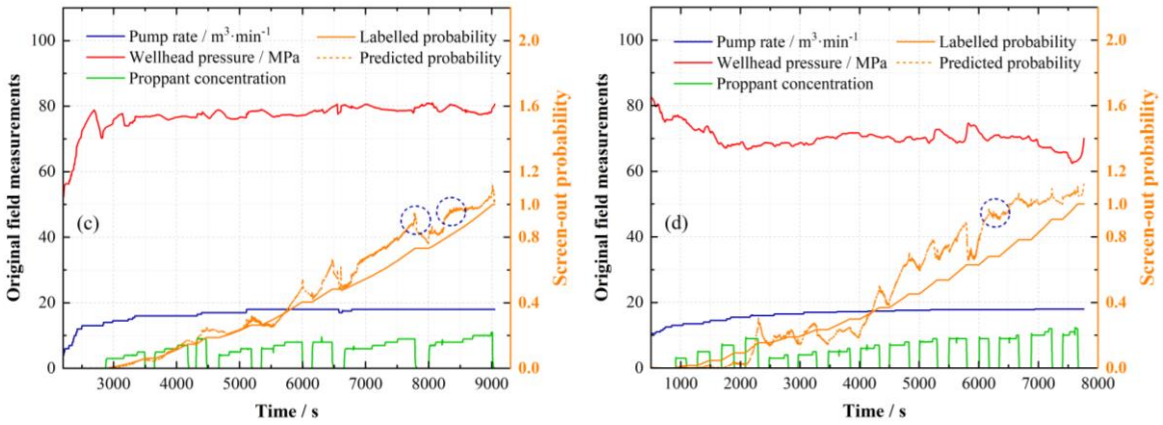

Fig. 3 Promoted predictions of screen-out probability by model inputs optimization based on (a) Well A, (b) Well B, (c) Well C and (d) Well D. The inputs of the model are consist of the original measurements and three optimized indicators (V_s/V_f + DPP + $\Delta P/\Delta V_f$). The blue dashed circle marks the false alarm of the screen-out in the Wells C and D cases. The solid orange line is the labelled screen-out probability curve. The dashed line is the predicted probability curve.

4 Discussion

4.1 Inducement analysis based on continuous probability

The probability curve before the screen-out also provides clues for the inducement analysis. In Fig. 3 (a), the long proppant injection slug between 4000s and 5000s increases the screen-out probability near to the value of 0.8, indicating that the continuous-proppant-injection length may be one of the key factors causing the screen-out in this case. In Fig. 3 (b), a vertical ascent of probability is observed around 3000s, when the 40/70 mesh proppant is injected right after the 100 mesh one. The fracture may not be well cracked with a relatively narrow width that is sensitive to larger proppant grain. The underdeveloped fracture may be an important inducement for Well B. The pressure fluctuations in Well A and B also show similar periods to the probability variations.

For Wells C and D, the sign showing in pressure is inconspicuous because it deviates only slightly from the norm, as shown in Figs. 3 (c) and (d). The probability can still define distinct indications precursory to screen-out. A long proppant slug may be one of the main reasons causing the screen-out in Well C, according to the rapid climb in probability between 6000s and 8000s in Fig. 3 (c). Meanwhile, a different mechanism prompting screen-out is disclosed in Well D. The probability begins increasing after 2000s when four slugs of fine proppant (100 mesh) are injected. In the 7th, 8th,

11^{th} and 12^{th} proppant slugs, 100 and 40/70 mesh proppants are successively injected (the short vertical lines in the middle of those concentration curves denote the switching between proppants), which all cause significant fluctuations in the probability curve at ~4000s and ~6000s. Conceivably, fine proppant may have filled micro- and secondary fractures, which should be beneficial to the stimulation. However, the 30/50 mesh proppant, not commonly used due to its large size, is injected during the last slug. The larger diameter proppant builds pressure in the main fractures, which may be difficult to be relieved as a result of staunched flow through the fully-packed minor fractures - hence triggering a screen-out.

According to the inducement analyses, the proppant may be injected slower to control the slug length for Wells A and C. Larger proppant may be switched later to allow a sufficient propagation of fracture for Well B. The amount of fine proppant should be controlled, especially when large diameter proppant is employed for Well D. However, adopting fine-grained proppant can be a double-edged sword. Certainly, it fills the minor fractures and boosts the growth of main fractures by increasing the net pressure. However, conversely, it may also reduce the pressure tolerance and increase the probability of screen-out, thus should be used with caution.

4.2 Support of the screen-out hypotheses

The predicted probability of screen-out varies in a similar period to the wellhead pressure variations (Fig. 3), indicating that the GRU model interprets the relationship between wellhead pressure and screen-out events when the data are manually trimmed. The predicted curves fluctuate around the labelled curves due to the finite and substantial variation in evolving fracture volume, which supports the linear hypothesis of screen-out probability. In addition, the V_s/V_f ratio represents the proppant accumulation in downhole fractures. The *DPP* and $\Delta P/\Delta V_f$ variations could result from the pressure response to fracture creation and propagation. The combination of these indicators significantly promotes predictions, which supports the determining elements hypothesis.

Additionally, the variation of underground fracture is currently difficult to detect and is a non-directly-adjustable parameter. Proppant accumulation may be the most significant indicative element considering the RMSE improvement in Table 5. Pumping rate is the single most important element that may be adjusted to ensure the operation safety. Emergency termination or reduction in pumping

rate is commonly used to control the pressure when the first signs of screen-out appear (Yew and Weng 2014). Therefore, it is essential to reveal the effect of pump rate on screen-out probability based on both training and testing datasets.

4.3 Effect of pump rate on screen-out probability

A U-shaped correlation between pump rate and screen-out is proposed according to the observation that both extremely low (aggravating the proppant settling and dune building-up) and extremely high (increasing the frictions and reshape the proppant dune) pump rates may result in sand screen-out (Harris and Pippin 2000; Willingham, Tan, and Norman 1993). This is demonstrated by fitting the correlation between the square-of-pump-rate with screen-out probability in STATA bases on both training and testing datasets. A small p-value (a smaller p-value reflects stronger evidence in favour of the hypothesis) and a positive coefficient are obtained, as shown in Table 6, which supports the U-shaped form hypothesis.

Table 6 Summary of regressions between the squared pump rate and screen-out probability

Dependent variable	Screen-out probability		
Independent variables	Pump rate		-0.042***
	Squared pump rate		**0.003*** **
Control variables	Mini-horizontal-stress	-0.021***	-0.014***
	Stage length	0.004***	0.002***
	Fluid viscosity	-0.005***	-0.003***
	Proppant concentration	0.817***	0.700***
	Proppant diameter	0.003***	-0.007***
	Wellhead pressure	0.010***	0.010***
Constant		0.328***	0.281***
R-squared		0.442	0.501

Notes: *** p<0.01, ** p<0.05, * p<0.1.

A flat U-shaped curve is observed with a minimum where the screen-out probability is lowest, as shown in Fig. 4. The pump rate at this minimum probability is 5.94 m^3/min based on the collected data in this work, which is defined as the safest fracturing pump rate (SFPR). An adjustment in pump rate is one of the most essential and frequent measures to maintain pressure and ensure safety during shale gas fracturing (Yew and Weng 2014). The newly defined SFPR can be used as a reference for

the real-time pump rate adjustment, which may aid in rapidly reducing the pump rate to the safest range to prevent or mitigate screen-out.

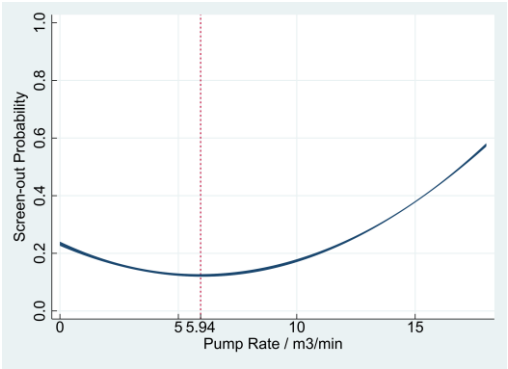

Fig. 4 U-shaped correlation between squared pump rate and screen-out probability. The vertical dashed line marks the pump rate at the turning point, which is 5.94 m^3/min.

The moderating effects of in-situ stress on the SFPR are studied based on both the low(er) and high(er) stress datasets, split by the median value (55 MPa) of the minimum-horizontal stress. These results are presented in Fig. 5. The SFPR moves rightward under the low-stress condition and grows to 8.33 m^3/min at the minimum probability. This reduces to 4.25 m^3/min for high(er)-stress conditions. In addition, the U-shaped curve is steeper for the low-stress condition, indicating that the probability of screen-out is more sensitive to a variation in pump rate and that the lifting of pump rate should be pursued with moderation. It is noteworthy that the SFPR may not be the most effective choice in practice since the operator may be willing to take certain risks to improve the economics of the stimulation job. However, it could be an important index to prompt pump rate adjustment to minimize loss when the first signs of the screen-out appear.

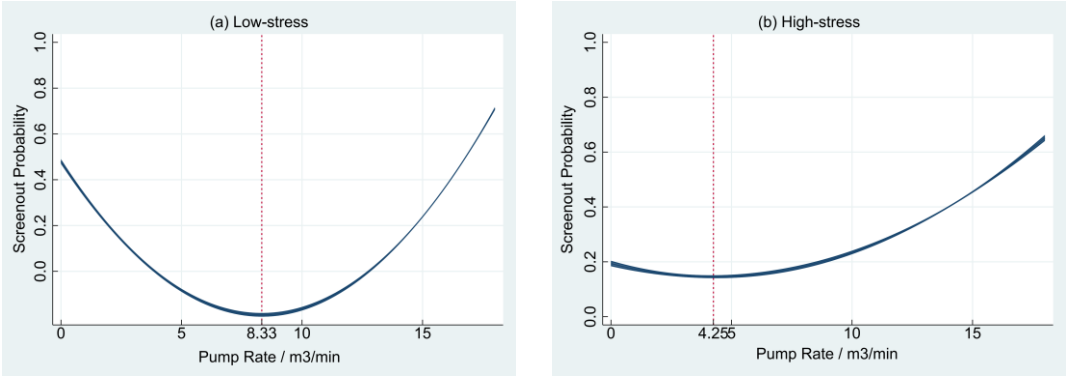

Fig. 5 Moderating effects of in-situ stress on the U-shape correlation. The vertical dashed line marks the extreme point excursion under (a) low-stress and (b) high-stress conditions. The pump rates at the turning points are 8.33 and 4.25 m^3/min, respectively.

5 Conclusions

A new awareness of screen-out mechanisms is highlighted by proposing and testing hypotheses based on a deep learning (GRU algorithm) workflow and the STATA software. Shale gas fracturing measurements are collected with a strict definition of screen-out applied (when the operation is suspended for pressure-release and wellbore-cleaning) to allow the binning of data. Time histories of fracturing parameters are truncated after screen-out to force the GRU model to interpret the pre-screen-out data – this is shown to improve the prediction of screen-out occurrences. A forward selection strategy is applied to optimize the model inputs, based on which accurate screen-out probability predictions are obtained. The major conclusions may be generalized as follows:

(1) By tuning the GRU model and optimizing the inputs, an accurate screen-out probability is produced in the testing cases for wells at different distances from the training wells. The GRU-based workflow successfully reports all the screen-out events and constrains the RMSE to ~0.089. The resulting continuous probability curve aid the field engineer to effectively monitor the evolution of screen-out, make rapid pre-judgements and prescribe mitigating actions in real-time. Besides, the variation in probability precursory to screen-out provides valuable clues regarding triggering mechanisms. For example, the length of the proppant slug, the timing of the switching of proppant sizes and the use of fine proppant are analyzed for the testing cases based on the evolution of the probability curves. Explicit strategies are proposed for optimizing the proppant selection and injection.

(2) Fracture volume, proppant accumulation and pump rate are proposed as three discriminating elements potentially contributing to screen-out, with these applied in data pre-processing in the workflow. This presumption is supported by producing the smallest prediction errors in the optimization of model inputs. Unique features of the mismatch among these elements may provide simple diagnostics for the mechanism of screen-out for shale gas fracturing. Fracture volume is a non-directly-adjustable parameter that may be reflected by the pressure variations. Proppant accumulation may be a significant indicative parameter for screen-out. Pumping rate is shown to be the most important adjustable element that controls the fracturing pressure. This three-determining-element

mechanism extends the characteristic parameters for screen-out study compared with traditional methods depending on pressure interpretation or proppant accumulation.

(3) A safest-fracturing pump rate (SFPR) is defined by fitting the U-shaped correlation between the screen-out probability and pump rate – this is 5.94 m^3/min based on the collected data. The moderating effect of in-situ stress on the SFPR shows that conditions of higher-stress reduce the SFPR. Conditions of lower-stress increase the SFPR, but also increase the relief of the U-shaped relation, indicating a higher sensitivity to pump rate that requires only a moderate adjustment. The SFPR may be used as a reference to guide the rapid adjustment of the pump rate into the safest range to potentially mitigate screen-out.

Acknowledgement

This research has received funding from the European Union's Horizon 2020 research and innovation programme under the Marie Sklodowska-Curie grant agreement No. 846775.

References

Aud, WW, TB Wright, CL Cipolla, and JD Harkrider. 1994. The effect of viscosity on near-wellbore tortuosity and premature screenouts. Paper presented at the SPE annual technical conference and exhibition, New Orleans, Louisiana, USA, 25–28 September. SPE-28492-MS. https://doi.org/10.2118/28492-MS.

Barree, RD, and MW Conway. 2001. Proppant holdup, bridging, and screenout behavior in naturally fractured reservoirs. Paper presented at the SPE Production and Operations Symposium, Oklahoma City, Oklahoma, USA, 24–27 March. SPE-67298-MS. https://doi.org/10.2118/67298-MS.

Ben, Yuxing, Michael Perrotte, Mohammadmehdi Ezzatabadipour, Irfan Ali, Sathish Sankaran, Clayton Harlin, and Dingzhou Cao. 2020. Real time hydraulic fracturing pressure prediction with machine learning. Paper presented at the SPE Hydraulic Fracturing Technology Conference and Exhibition, The Woodlands, Texas, USA, 4–6 February. SPE-199699-MS. https://doi.org/10.2118/199699-MS.

Benesty, Jacob, Jingdong Chen, Yiteng Huang, and Israel Cohen. 2009. Pearson correlation coefficient. In *Noise reduction in speech processing*, 1-4. Springer.

Bergstra, James, and Yoshua Bengio. 2012. Random search for hyper-parameter optimization. *Journal of machine learning research* 13 (2).

Cai, Xiao, Boyun Guo, Gao Li, and Xu Yang. 2017. A Semi Analytical Model for Predicting Proppant Screen-Out During Hydraulic Fracturing Unconventional Reservoirs. Paper presented at the SPE/IATMI Asia Pacific Oil & Gas Conference and Exhibition, Jakarta, Indonesia, 17–19 October. SPE-186174-MS. https://doi.org/10.2118/186174-MS.

Chai, Tianfeng, and Roland R Draxler. 2014. Root mean square error (RMSE) or mean absolute error (MAE)?–Arguments against avoiding RMSE in the literature. *Geoscientific model development* 7 (3): 1247-1250. https://doi.org/10.5194/gmd-7-1247-2014.

Cho, Kyunghyun, Bart Van Merriënboer, Caglar Gulcehre, Dzmitry Bahdanau, Fethi Bougares, Holger Schwenk, and Yoshua Bengio. 2014. Learning phrase representations using RNN encoder-decoder for statistical machine translation. *arXiv preprint arXiv:1406.1078*.

Cleary, MP, DE Johnson, HH Kogsbøll, KA Owens, KF Perry, CJ De Pater, Alfred Stachel, Holger Schmidt, and Tambini Mauro. 1993. Field implementation of proppant slugs to avoid premature screen-out of hydraulic fractures with adequate proppant concentration. Paper presented at the Low Permeability Reservoirs Symposium, Denver, Colorado, USA, 26–28 April. SPE-25892-MS. https://doi.org/10.2118/25892-MS.

Dahi-Taleghani, Arash, and Jon E Olson. 2011. Numerical modeling of multistranded-hydraulic-fracture propagation: accounting for the interaction between induced and natural fractures. *SPE journal* 16 (03): 575-581. SPE-124884-PA. https://doi.org/10.2118/124884-PA.

Daneshy, A Ali. 2007. Pressure variations inside the hydraulic fracture and their impact on fracture propagation, conductivity, and screenout. *SPE Production & Operations* 22 (01): 107-111. SPE-95355-PA. https://doi.org/10.2118/95355-PA.

Dontsov, E. V, and A. P Peirce. 2014. Slurry flow, gravitational settling and a proppant transport model for hydraulic fractures. *Journal of Fluid Mechanics* 760: 567-590. https://doi.org/10.1017/jfm.2014.606.

Dontsov, EV, and AP Peirce. 2015. Proppant transport in hydraulic fracturing: crack tip screen-out in KGD and P3D models. *International Journal of Solids and Structures* 63: 206-218. https://doi.org/10.1016/j.ijsolstr.2015.02.051.

Economides, Michael J, and Kenneth G Nolte. 1989. *Reservoir stimulation*. Vol. 2. Prentice Hall Englewood Cliffs, NJ.

Fan, Dongyan, Hai Sun, Jun Yao, Kai Zhang, Xia Yan, and Zhixue Sun. 2021. Well production forecasting based on ARIMA-LSTM model considering manual operations. *Energy* 220. https://doi.org/10.1016/j.energy.2020.119708.

Gal, Yarin, and Zoubin Ghahramani. 2015. A theoretically grounded application of dropout in recurrent neural networks. *arXiv preprint arXiv:1512.05287*.

Harris, PC, and PM Pippin. 2000. High-rate foam fracturing: fluid friction and perforation erosion. *SPE Production & Facilities* 15 (01): 27-32. SPE-60841-PA. https://doi.org/10.2118/60841-PA.

Hayashi, Kazuo, and Bezalel C Haimson. 1991. Characteristics of shut-in curves in hydraulic fracturing stress measurements and determination of in situ minimum compressive stress. *Journal of Geophysical Research: Solid Earth* 96 (B11): 18311-18321. https://doi.org/10.1029/91JB01867.

Hu, Jinqiu, Faisal Khan, Laibin Zhang, and Siyun Tian. 2020. Data-driven early warning model for screenout scenarios in shale gas fracturing operation. *Computers & Chemical Engineering* 143. https://doi.org/10.1016/j.compchemeng.2020.107116.

Hu, Michael Y, Guoqiang Zhang, Christine X Jiang, and B Eddy Patuwo. 1999. A cross-validation analysis of neural network out-of-sample performance in exchange rate forecasting. *Decision Sciences* 30 (1): 197-216. https://doi.org/10.1111/j.1540-5915.1999.tb01606.x.

Kingma, Diederik P, and Jimmy Ba. 2014. Adam: A method for stochastic optimization. *arXiv preprint arXiv:1412.6980*.

Li, Quanshu, Huilin Xing, Jianjun Liu, and Xiangchon Liu. 2015. A review on hydraulic fracturing of unconventional reservoir. *Petroleum* 1 (1): 8-15. https://doi.org/10.1016/j.petlm.2015.03.008.

Manchanda, Ripudaman, Shuang Zheng, Sho Hirose, and Mukul M Sharma. 2020. Integrating reservoir geomechanics with multiple fracture propagation and proppant placement. *SPE Journal*25 (02): 662–691. SPE-199366-PA. https://doi.org/10.2118/199366-PA.

Massaras, Leon V, and Dimitri V Massaras. 2012. Real-time Advanced Warning of Screenouts with the Inverse Slope Method. Paper presented at the SPE International Symposium and Exhibition on Formation Damage Control, Lafayette, Louisiana, USA, 15–17 February. SPE-150263-MS. https://doi.org/10.2118/150263-MS.

Merry, Hoagie, and Panayiotis Dalamarinis. 2020. Multi-Basin Case Study of Real-Time Perforation Quality Assessment for Screen Out Mitigation and Treatment Design Optimization Using Tube Wave Measurements. Paper presented at the SPE Annual Technical Conference and Exhibition, Virtual, 26–29 October. SPE-201686-MS. https://doi.org/10.2118/201686-MS.

Nolte, Kenneth G, and Michael B Smith. 1981. Interpretation of fracturing pressures. *Journal of Petroleum Technology* 33 (09): 1767-1775. SPE-8297-PA. https://doi.org/10.2118/8297-PA.

Novotny, EJ. 1977. Proppant transport. Paper presented at the SPE Annual Fall Technical Conference and Exhibition, Denver, Colorado, USA, 7–19 October. SPE-6813-MS. https://doi.org/10.2118/6813-MS.

Patankar, Neelesh A, DD Joseph, J Wang, RD Barree, M Conway, and M Asadi. 2002. Power law correlations for sediment transport in pressure driven channel flows. *International Journal of Multiphase Flow* 28 (8): 1269-1292. https://doi.org/10.1016/S0301-9322(02)00030-7.

Pounds, Stan, and Stephan W Morris. 2003. Estimating the occurrence of false positives and false negatives in microarray studies by approximating and partitioning the empirical distribution of p-values. *Bioinformatics* 19 (10): 1236-1242. https://doi.org/10.1093/bioinformatics/btg148.

Qi, Wu, Xu Yun, Wang Xiaoquan, Wang Tengfei, and Shouliang Zhang. 2012. Volume fracturing technology of unconventional reservoirs: Connotation, design optimization and implementation. *Petroleum Exploration and Development* 39 (3): 377-384. https://doi.org/10.1016/S1876-3804(12)60054-8.

Roussel, Nicolas Patrick, Ripudaman Manchanda, and Mukul Mani Sharma. 2012. Implications of fracturing pressure data recorded during a horizontal completion on stage spacing design. Paper presented at the SPE Hydraulic Fracturing Technology Conference, The Woodlands, Texas, USA, 6–8 February. SPE-152631-MS. https://doi.org/10.2118/152631-MS.

Sagheer, Alaa, and Mostafa Kotb. 2019. "Time series forecasting of petroleum production using deep LSTM recurrent networks." *Neurocomputing* 323: 203-213. https://doi.org/10.1016/j.neucom.2018.09.082.

Stein, Roger M. 2002. Benchmarking default prediction models: Pitfalls and remedies in model validation. *Moody's KMV, New York* 20305.

Sun, Jianlei John, Arvind Battula, Brandon Hruby, and Paymon Hossaini. 2020. Application of Both Physics-Based and Data-Driven Techniques for Real-Time Screen-Out Prediction with High Frequency Data. Paper presented at the SPE/AAPG/SEG Unconventional Resources

Technology Conference, Virtual, 20–22 July. URTEC-2020-3349-MS. https://doi.org/10.15530/urtec-2020-3349.

Wang, Jinjiang, Jianxing Yan, Chen Li, Robert X. Gao, and Rui Zhao. 2019. Deep heterogeneous GRU model for predictive analytics in smart manufacturing: Application to tool wear prediction. *Computers in Industry* 111: 1-14. https://doi.org/10.1016/j.compind.2019.06.001.

Warpinski, Norman Raymond, Michael J Mayerhofer, Michael C Vincent, Craig L Cipolla, and EP Lolon. 2009. Stimulating unconventional reservoirs: maximizing network growth while optimizing fracture conductivity. *Journal of Canadian Petroleum Technology* 48 (10): 39-51. SPE-114173-PA. https://doi.org/10.2118/114173-PA.

Weng, Xiaowei, Olga Kresse, Charles Edouard Cohen, Ruiting Wu, and Hongren Gu. 2011. Modeling of hydraulic fracture network propagation in a naturally fractured formation. *SPE Production & Operations* 26 (04): 368–380. SPE-140253-PA. https://doi.org/10.2118/140253-PA.

Willingham, JD, HC Tan, and LR Norman. 1993. Perforation friction pressure of fracturing fluid slurries. Paper presented at the Low Permeability Reservoirs Symposium, Denver, Colorado, USA. 26–28 April. SPE-25891-MS. https://doi.org/10.2118/25891-MS.

Yew, Ching H, and Xiaowei Weng. 2014. *Mechanics of hydraulic fracturing*. Gulf Professional Publishing.

Yu, Xiaodan, Whitney Trainor-Guitton, and Jennifer Miskimins. 2020. A Data Driven Approach in Screenout Detection for Horizontal Wells. Paper presented at the SPE Hydraulic Fracturing Technology Conference and Exhibition, The Woodlands, Texas, USA, 4–6 February. SPE-199707-MS. https://doi.org/10.2118/199707-MS.

Zeiler, Matthew D. 2012. Adadelta: an adaptive learning rate method. *arXiv preprint arXiv:1212.5701*.